JGR Oceans

RESEARCH ARTICLE
10.1029/2024JC021271

Wind-Driven Along-Coast Pressure Gradients in the Middle Atlantic Bight

Steven J. Lentz[1]

[1]Physical Oceanography, Woods Hole Oceanographic Institution, Woods Hole, MA, USA

Key Points:

- Along-shelf wind stresses setup substantial along-coast pressure gradients in the Middle Atlantic Bight at time scales from days to years
- The along-coast pressure gradients tend to oppose the wind stress and are driven by both local and remote wind stresses
- A steady, depth-averaged, barotropic model proposed by Csanady (1978) accurately reproduces the observed along-coast pressure gradients

Correspondence to:

S. J. Lentz,
slentz@whoi.edu

Citation:

Lentz, S. J. (2024). Wind-driven along-coast pressure gradients in the Middle Atlantic Bight. *Journal of Geophysical Research: Oceans*, *129*, e2024JC021271. https://doi.org/10.1029/2024JC021271

Received 25 APR 2024
Accepted 31 AUG 2024

Author Contribution:

Conceptualization: Steven J. Lentz
Data curation: Steven J. Lentz
Formal analysis: Steven J. Lentz
Investigation: Steven J. Lentz
Methodology: Steven J. Lentz
Resources: Steven J. Lentz
Software: Steven J. Lentz
Validation: Steven J. Lentz
Writing – original draft: Steven J. Lentz
Writing – review & editing: Steven J. Lentz

Abstract Along-shelf wind stresses drive substantial along-coast variations in sea level that result in significant along-coast pressure gradients in the Middle Atlantic Bight (MAB) at time scales from days to years. Forty years of sea-level data and reanalysis wind stresses are examined to determine the characteristics and dynamics of pressure gradients along the New England and Central MAB coasts. Along-coast dynamic sea level (pressure) gradients often exceed 5 cm/100 km at daily time scales, 2 cm/100 km at monthly time scales and 0.2 cm/100 km at yearly time scales. Along-shelf wind stresses account for more than 50% of the along-coast pressure gradient variance at daily and monthly time scales and more than 25% at yearly time scales. Pressure gradients along the New England coast are primarily driven by local wind stresses along the New England shelf, while pressure gradients along the Central MAB shelf are driven by both local wind stresses along the Central MAB shelf and remote wind stresses along the New England shelf. A steady depth-average model (Csanady, 1978, https://doi.org/10.1175/1520-0485(1978)008<0047:tatw>2.0.co;2) accurately reproduces the wind-driven along-coast pressure gradients in both regions. The along-coast pressure gradients typically oppose the local wind stress and, in the along-shelf momentum balance, are 50%–80% of the along-shelf wind stress over the inner shelf (water depth 15 m).

Plain Language Summary Along-coast variations in the wind-driven set up or set down of coastal sea level results in along-coast pressure gradients that are an important part of the dynamics that establish currents over the continental shelf. Coastal sea level from tide gauges along the East Coast of the United States from North Carolina to Massachusetts for the 40 year period from 1982 to 2021 are used to estimate the along-coast pressure gradients and investigate their characteristics. The established along-coast pressure gradients tend to oppose the local wind stress and consequently reduce the strength of the resulting along-shelf currents. However, along-coast pressure gradients are also driven by winds to the north and east of the tide gauge because of a tendency for sea level variations to preferentially spread along the coast from the northeast toward the southwest. This component of the along-coast pressure gradient forces along-shelf currents caused by remote wind forcing. A simple, wind-forced, model that includes this remote forcing accurately reproduces the observed coastal pressure gradients.

1. Introduction

A key element of the wind-driven response of continental shelves is the development of along-shelf pressure gradients that arise because of along-shelf variations in the wind field and the bathymetry. In coastal regions dominated by local wind forcing the along-shelf pressure gradient typically opposes the wind stress and consequently reduces the along-shelf current response (Allen & Smith, 1981; Brown et al., 1987; Fewings & Lentz, 2010; Gutierrez et al., 2006; Lee et al., 1984, 1989; Lentz, 1994, 2022; Li et al., 2014; Liu & Weisberg, 2005; Masse, 1988; McCabe et al., 2015; Noble et al., 1983; Ofsthun et al., 2019; Pettigrew, 1981; Shearman & Lentz, 2003). Along-shelf wind forcing can also impact remote coastal regions through long coastal-trapped waves that propagate in only one direction alongshore (with the coast on the right in the Northern Hemisphere) (e.g., Brink, 1991). The resulting along-shelf pressure gradients driven by remote wind forcing can be a dominant component of the along-shelf current dynamics in some regions (Allen & Smith, 1981; Hickey, 1984; Hickey & Pola, 1983; Hickey et al., 2003; Kirincich & Barth, 2009; Lentz & Winant, 1986; Noble et al., 2002). Consequently, the wind-driven sea-level response that generates both local and remote along-shelf pressure gradients is a critical element of subtidal dynamics on most continental shelves.

The focus of this study is the Middle Atlantic Bight (MAB) continental shelf which is characterized by an abrupt change in the coastline orientation at Sandy Hook, between the New England and Central MAB shelves

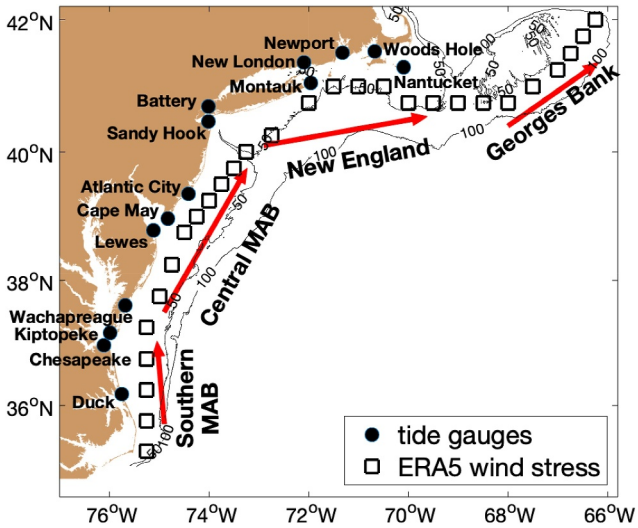

Figure 1. Map of the Middle Atlantic Bight (MAB) and Georges Bank showing the locations of tide gauges and the mid-shelf ERA5 wind stresses. The red arrows indicate the direction of the along-shelf wind stress in the four shelf regions. Pressure gradients along the New England and Central MAB coasts are estimated from the tide gauge sea levels.

(Figure 1). Early studies established the development of pressure gradients along the New England coast and their impact on the dynamics. Beardsley and Butman (1974) observed a sea-level difference of 60 cm between Nantucket and Sandy Hook in response to strong eastward winds during a storm in March 1973. Several subsequent studies showed the consistent development of pressure gradients along the New England coast that opposed east-west along-shelf wind stresses (e.g., Beardsley et al., 1977; Chase, 1979; Noble & Butman, 1979; Wang, 1979). Numerous studies have also shown that at time scales of days to weeks along-shelf current variability over the MAB is primarily wind driven, that along-shelf pressure gradients are an important component of the dynamics and that along-shelf pressure gradients often oppose the wind stress (e.g., Bennett & Magnell, 1979; Fewings & Lentz, 2010; Lentz, 2022; Lentz et al., 1999; Masse, 1988; Noble et al., 1983; Ofsthun et al., 2019; Pettigrew, 1981; Shearman & Lentz, 2003). These studies have focused on the local dynamics at specific sites in the MAB. Consequently, there is not a consistent, comprehensive picture of along-shelf pressure gradient characteristics in the MAB, the associated dynamics and whether the along-shelf pressure gradients are locally or remotely forced.

The wind-driven response of pressure gradients along the New England and Central MAB coasts at time scales from days to years is examined here using 40 years of coastal sea-level measurements to estimate along-coast pressure gradients and ECMWF ERA5 reanalysis wind stresses over Georges Bank and in the MAB (Figure 1). The primary objectives are to determine: (a) the characteristics of the along-coast pressure gradient response to along-shelf wind stress at time scales of days, months and years; (b) the relative importance of local vs. remote wind forcing in setting up pressure gradients along the New England and Central MAB coasts; and (c) the fundamental dynamics and the key parameters influencing the wind-driven response of along-coast pressure gradients. A steady, linear, depth-average model (Arrested Topographic Wave) proposed by Csanady (1978) is used to aid in the interpretation of the observations and addressing the primary objectives, particularly objective 3. A companion paper examines the wind-driven response of sea level along the MAB coast (Lentz, 2024).

2. Data and Processing

Hourly sea-level measurements from 14 NOAA tide gauges and 3-hourly wind stresses from the European Centre for Medium-Range Weather Forecasts (ECMWF) global reanalysis ERA5 on a 1/4° grid (Hersbach et al., 2023) are used to characterize the along-coast pressure gradient response to wind stress in the MAB for the 40-year period from 1982 through 2021. The ERA5 wind stresses provide complete spatial and temporal coverage and are an accurate representation of wind stresses estimated from NDBC buoy measurements (Lentz, 2024).

Based on the notion that the along-coast pressure gradient response is primarily due to along-shelf wind stresses, the MAB is divided into three regions separated by changes in coastline/isobath orientation: the New England, Central MAB, and Southern MAB shelves (Figure 1). Additionally, wind stresses over the Southern Flank of Georges Bank are included to account for some of the remote, poleward forcing. The along-shelf wind stress directions in each region are: Georges Bank 55°T (clockwise from true north); New England 80°T; Central MAB 30°T; and Southern MAB −5°T (Figure 1 red arrows). Mid-shelf ERA5 grid points are used to represent the along-shelf wind stress, so cross-shelf variations in the along-shelf wind stress are not considered. There is an implicit assumption that over the shallow crest of Georges Bank strong tidal currents drive large turbulent stresses that block the cross-isobath wind-driven Ekman transport similar to a coastal wall (e.g., Noble et al., 1985; Wright et al., 1986). The choice to extend the wind forcing to the Southern Flank of Georges Bank, but not farther north is based on: (a) the practical need to pick a northward limit to the model; (b) the continuity of the isobaths and shelf flow over Georges Bank Southern Flank and the New England shelf (e.g., Noble & Butman, 1979; Noble et al., 1983); and (c) the presumed inability of the simple ATW model to reproduce the complexity of the wind-driven barotropic response in the Gulf of Maine (e.g., Greenberg et al., 1997; Pringle, 2006; Wright et al., 1986). The impact of excluding forcing poleward of the Southern Flank of Georges Bank is briefly discussed in Section 5.

Pressure gradients are characterized in terms of dynamic sea level $\eta^P = \eta^{sl} + P^A/\rho_o g$, which is estimated by interpolating the ERA5 atmospheric pressures P^A to the tide gauge locations (ρ_o is ocean density and g is gravity). The hourly sea-level time series have the mean removed and are detided prior to computing along-coast pressure gradients and daily, monthly, and yearly averages (see Lentz, 2024 for more details on the observations). Along-coast pressure gradients for the New England and Central MAB regions are estimated by a linear regression of dynamic sea level versus along-coast distance. For the New England shelf there are 7 tide gauges (Nantucket to Sandy Hook), but essentially only 5 separate sites, since Montauk, New London and Battery, Sandy Hook are at approximately the same along-shelf locations. For the Central MAB there are 6 tide gauges (Battery to Chesapeake Bay). Only stations with data at a given time are included in the linear regression analysis. There is not an observational estimate of the along-coast pressure gradient in the Southern MAB because there is only one tide gauge (Duck). The linear regression analyses yield regional scale (order 500 km) estimates of the along-coast pressure gradient. More spatially refined estimates of the along-shelf pressure gradient using pairs of tide gauges were too noisy to be useful, presumably because of uncertainties in the measurements and local sea-level variations associated with individual tide gauge stations.

3. The Arrested Topographic Wave Model

Csanady (1978) showed that for the steady, barotropic, depth-average equations, assuming volume conservation, a geostrophic cross-shelf momentum balance, and a linear along-shelf momentum balance including a linear drag law relating the bottom stress to the depth-average current, could be reduced to a diffusion equation for the sea-level variations

$$\frac{\partial \eta_P}{\partial y} + L_r \frac{\partial^2 \eta_P}{\partial^2 x} = 0, \text{ where } L_r = \frac{r}{f \partial h/\partial x}. \tag{1}$$

Here x is cross-shelf, y is along-shelf, $\partial h/\partial x$ is the cross-shelf bottom slope, f is the Coriolis parameter, and r is a linear drag coefficient. A key feature of Equation 1 is that the sea level response to the along-shelf wind stress forcing only spreads in the direction of long coastal-trapped wave propagation (the negative y direction, for the MAB this is equatorward). The "diffusion" coefficient, L_r, is a length scale relating the cross-shelf and along-shelf scales of the response. Consistent with vorticity constraints, the offshore diffusion (L_r) of the response is enhanced by the bottom drag, r, and inhibited by the Coriolis, f, and cross-shelf bottom slope, $\partial h/\partial x$. For an along-shelf length scale L_y the cross-shelf length scale of the response is $L_{ATW} = \sqrt{L_r L_y}$. The corresponding water depth scale is

$$D_{\mathrm{ATW}} = L_{\mathrm{ATW}} \frac{\partial h}{\partial x} = \sqrt{\frac{L_y\, r\, \partial h/\partial x}{f}} \tag{2}$$

Csanady (1978) provides an analytic solution to Equation 1 for a semi-infinite (offshore) shelf with a constant bottom slope, forced by a constant along-shelf wind stress τ^{sy} over the region from $-L_y \le y \le 0$ and zero along-shelf wind stress for $y < -L_y$. Sea level at the coast is

$$\eta^P(\tilde{x}=0) = -\frac{2}{\sqrt{\pi}} \frac{\tau^{sy}}{\rho g} \frac{f L_{\mathrm{ATW}}}{r} \tilde{y}^{1/2} \quad 0 \le \tilde{y} \le 1 = -\frac{2}{\sqrt{\pi}} \frac{\tau^{sy}}{\rho g} \frac{f L_{\mathrm{ATW}}}{r} \left\{ \tilde{y}^{1/2} - (\tilde{y}-1)^{1/2} \right\} \quad \tilde{y} > 1 \tag{3a}$$

and the along-coast pressure gradient at the coast is,

$$\frac{\partial \eta_{\mathrm{P}}(\tilde{x}=0)}{\partial y} = \frac{1}{\sqrt{\pi}} \frac{\tau^{sy}}{\rho_o g D_{\mathrm{ATW}}} \tilde{y}^{-1/2} \quad -1 \le \tilde{y} \le 0 = \frac{1}{\sqrt{\pi}} \frac{\tau^{sy}}{\rho_o g D_{\mathrm{ATW}}} \left\{ \tilde{y}^{-1/2} - (\tilde{y}-1)^{-1/2} \right\} \quad \tilde{y} < -1 \tag{3b}$$

(Figure 2 dashed lines). The along-coast pressure gradient only depends on the wind stress, the depth scale D_{ATW}, and the normalized along-shelf distance $\tilde{y} = y/L_y$. The along-coast pressure gradient is proportional to the wind stress and inversely dependent on the depth scale D_{ATW}. In the wind-forced region, the along-coast pressure gradient is positive and hence opposes the wind stress (Figure 2). In the unforced region, the pressure gradient has the opposite sign of the wind stress and drives an along-shelf current in the same direction as the remote wind forcing. For this analytic solution, there are singularities in the along-coast pressure gradient at the discontinuities

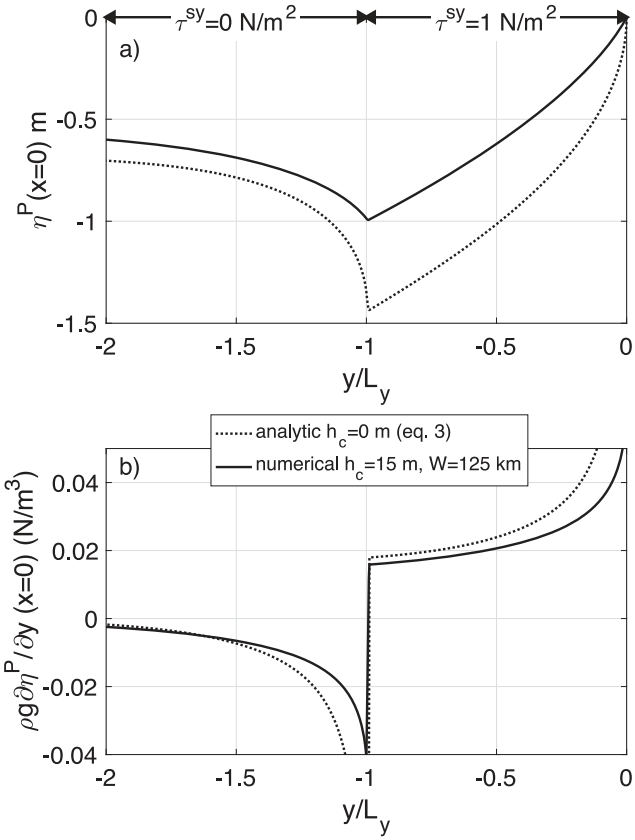

Figure 2. (a) Sea-level and (b) along-shelf pressure gradient response to a constant wind stress over a region of length L_y from ATW model. The analytic solution for an infinitely wide shelf with $h_c = 0$ (Equation 3; Csanady, 1978) and the numerical solution for a 125 km wide shelf with $h_c = 15$ m. In both cases, $f = 0.95 \times 10^{-4}$ s^{-1}, $\partial h/\partial x = 5 \times 10^{-4}$, and $r = 5 \times 10^{-4}$ m s^{-1}.

in the wind stress ($y/L_y = -1$ and 0, Figure 2) where the assumption that the along-shelf scale is large compared to the cross-shelf scale is not valid.

To incorporate the observed along-shelf wind stress forcing and more realistic bathymetry, Equation 1 is solved numerically using centered differences in the cross-shelf direction and forward differencing in the along-shelf direction. The approach and parameters are the same as described in Lentz (2024), so only a brief summary is given here. The model is forced by the daily averaged, mid-shelf, ERA along-shelf wind stresses using the along-shelf orientations noted in Section 2 (Figure 1). The model bathymetry is uniform along-shelf, with a 15 m deep coastal wall, a 125 km wide shelf with a constant bottom slope of $\partial h/\partial x = 0.0005$, and a 50 km wide continental slope, $\partial h/\partial x = 0.05$, based on the MAB bathymetry. Previous studies have used the ATW model with a coastal wall (Pettigrew, 1981) and a finite width shelf (Noble et al., 1983). The 15 m deep coastal wall causes a small reduction in the along-shelf pressure gradient at the coast (Figure 2b). The finite shelf width has little impact on the along-coast pressure gradient. The Coriolis parameter varies with latitude. The drag coefficient for Georges Bank and the eastern half of the Southern New England shelf, $r = 9 \times 10^{-4}$ m/s, is three times larger than in the rest of the MAB, $r = 3 \times 10^{-4}$ m/s, motivated by the stronger tidal currents over Georges Bank and the eastern half of the Southern New England shelf. For these parameters, the depth scale (Equation 2), D_x, is 37 m over Georges Bank and the New England shelf, 27 m over the Central MAB shelf and 17.5 m over the Southern MAB shelf.

4. Results

4.1. Along-Coast Pressure Gradient and Wind Stress Characteristics

Dynamic sea level (pressure) gradient variations along the New England and Central MAB coasts exhibit variability at time scales from days to years, with standard deviations of 2.5×10^{-7} (2.5 cm per 100 km) at daily time scales, 1×10^{-7} at monthly time scales and 0.4×10^{-7} at yearly time scales (Table 1). At time scales of days both along-coast wind stress and pressure gradient variability are larger in winter than in summer (e.g., Figure 3). During strong storms, dynamic sea-level differences along the New England coast (Nantucket to Sandy Hook), or the Central MAB coast (Sandy Hook to Chesapeake Bay), can exceed 50 cm. On the New England shelf, the along-coast pressure gradient is highly correlated with the local along-shelf component of the wind stress (Table 1, Figures 3a and 3b) and the regression coefficient is order 1 if the wind stress is scaled as in Equation 3b (Table 1). On the Central MAB shelf, the along-coast pressure gradient is less strongly correlated with the local along-shelf wind stress (Table 1, Figures 3c and 3d) with a scaled regression coefficient of order 1.

Table 1
Standard Deviations of the Observed Along-Coast Dynamic Sea Level Gradients, Correlations With the Along-Shelf Wind Stresses, the ATW Model Pressure Gradients and the Multiple Regression Analysis Regression Slopes for Daily, Monthly, and Yearly Averages for the New England (NE) and Central Middle Atlantic Bight (CMAB) Coasts

		Correlation			Regression slope	
	$\partial\eta^P/\partial y$ st. dev. ($\times 10^{-7}$)	$\frac{1}{\sqrt{\pi}}\frac{\tau^{sy}}{\rho g D_{ATW}}$	ATW model	Multiple regression	$\frac{1}{\sqrt{\pi}}\frac{\tau^{sy}}{\rho g D_{ATW}}$	ATW model
Daily NE	2.56	0.85	0.88	0.87	1.0 ± 0.01	0.87 ± 0.01
Monthly NE	1.12	0.89	0.90	0.90	1.3 ± 0.06	1.09 ± 0.05
Yearly NE	0.36	0.52	0.54	0.59	1.22 ± 0.66	1.09 ± 0.56
Daily CMAB	2.47	0.40	0.75	0.78	0.44 ± 0.17	0.88 ± 0.01
Monthly CMAB	0.80	0.62	0.81	0.80	0.82 ± 0.09	1.00 ± 0.07
Yearly CMAB	0.29	0.51	0.62	0.60	0.79 ± 0.44	1.16 ± 0.49

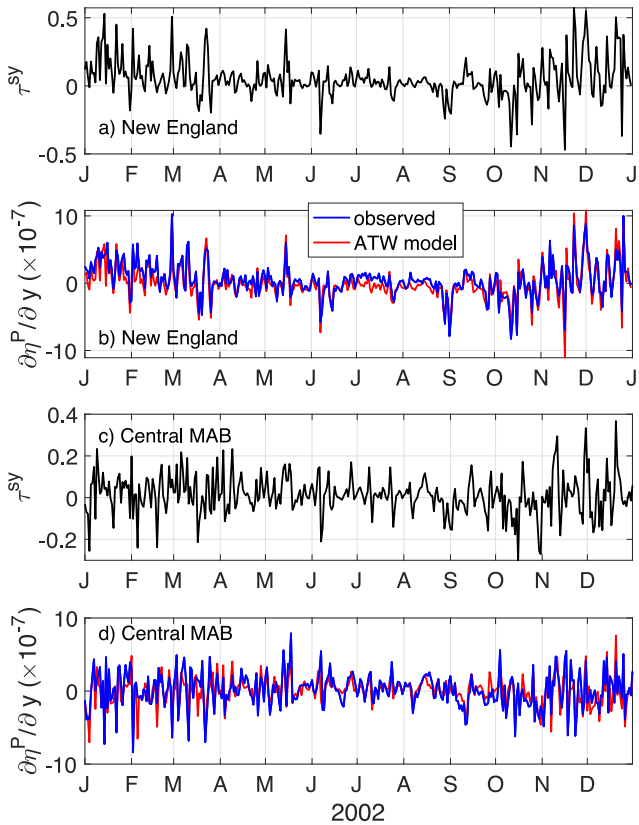

Figure 3. Daily along-shelf wind stresses (a, c) and observed and ATW model along-shelf pressure gradients (b, d) for the New England (a, b) and Central Middle Atlantic Bight (c, d) shelves in 2002.

Along-coast wind stresses over the New England and Central MAB shelves are moderately, positively correlated (0.50) at daily time scales, with clear differences during many storm events due primarily to the difference in orientation of the two coastlines. Along-coast pressure gradients in the two regions are weakly correlated (−0.35). The along-coast pressure gradients sometimes oppose each other and sometimes are in the same direction. For example, on 14 November 2003 (Figure 4a), when there was a strong eastward wind stress along the New England shelf and a weak wind stress along the Central MAB shelf the pressure gradients along the coast are in opposite directions. The sea level response is quantitatively similar to the boxcar wind forcing seen in Figure 2a (black line). In contrast, on 12 November 2009, there was a strong westward wind stress on the New England shelf and a strong southwestward wind stress on the Central MAB shelf resulting in an along-shelf pressure gradient in the same direction that spanned almost the entire MAB coast (Figure 4b). The weak negative correlation between along-coast pressure gradients in the two regions suggests the former example occurs a little more often than the latter.

At monthly time scales, the same relationships between the local along-shelf wind stress and along-coast pressure gradient hold as at daily time scales (Figure 5). Notably the local along-shelf wind stress and along-coast pressure gradients are highly correlated on the New England shelf and less correlated on the Central MAB shelf (Table 1). Relationships between the along-shelf wind stresses and along-coast pressure gradients in the two regions are also similar at monthly and daily time scales. At monthly time scales there is a substantial annual cycle on the New England shelf in the along-shelf wind stress and along-coast pressure gradient (Figures 5a, 5b, and 6a). The annual cycle of the pressure gradient along the New England coast is positive (sea level increasing eastward) in winter, negative in late spring and early fall, and close to zero in July (Figure 6a). The annual cycle of the pressure gradient along the Central MAB coast is positive (sea level increasing northward) in spring—summer with a maximum in July and negative in fall—winter. The phasing of the annual cycles of the pressure gradients are roughly consistent with the annual cycles of the along-shelf wind stress in each region (Figure 6 dashed lines), though the amplitude of the scaled along-shelf wind stress on the Central MAB shelf is about half the along-coast pressure gradient.

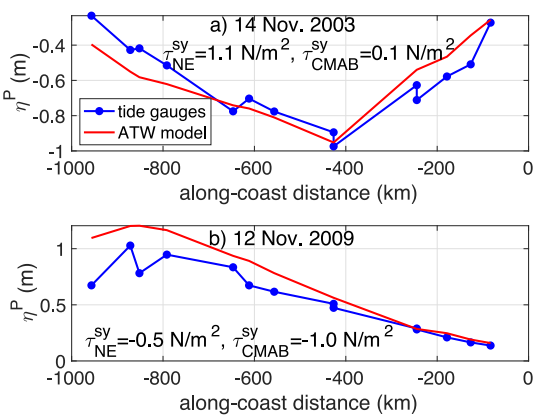

Figure 4. Examples of the along-coast variations in dynamic sea level in the Middle Atlantic Bight (MAB) during strong along-coast wind stresses on (a) 14 November 2003 and (b) 12 November 2009 from the tide gauges and the ATW model. Along-coast distance is relative to the eastern edge of the MAB.

At yearly time scales, correlations between the along-shelf wind stress and along-coast pressure gradient are lower (∼0.5) than at daily or monthly time scales (Table 1). Regression coefficients are still order 1 for the scaling given by Equation 3b. The lower correlations are almost certainly due in part to the smaller along-coast pressure gradient signal at yearly time scales relative to uncertainties in both the sea-level measurements and the gradient estimates (Section 5).

4.2. Local Versus Remote Forcing—Arrested Topographic Wave Model

Estimates of the along-coast pressure gradient from the Arrested Topographic Wave model, which includes both local and remote wind forcing, are highly correlated with the observed pressure gradients along both the New England and Central MAB coasts at daily and monthly time scales (Table 1, Figures 3–6 compare blue and red lines). At yearly time scales correlations are significant but smaller, presumably for the reasons noted in the previous section. For the New England shelf, the correlations are slightly higher for the ATW model than for the local along-shelf wind stress at daily, monthly, and yearly time scales (Table 1). For the Central MAB shelf, correlations are substantially larger for the ATW model than for the local along-shelf wind stress at

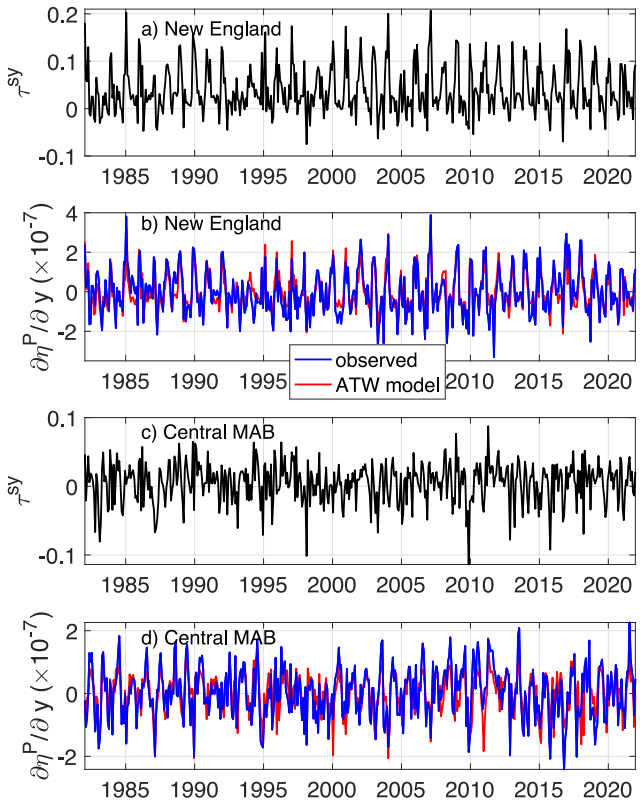

Figure 5. Monthly along-shelf wind stresses (a, c) and observed and ATW model along-shelf pressure gradients (b), (d) for the New England (a, b) and Central Middle Atlantic Bight (c, d) shelves.

daily, monthly, and yearly time scales. Regression coefficients are close to 1 for monthly and yearly time scales and slightly less than 1 for daily time scales. The regression coefficients at daily time scales are less than one because the ATW model tends to overestimate the along-coast pressure gradient during the strongest wind stress events (Figure 7). The slope of the relationship is close to 1 when the observed $|\partial\eta^P/\partial y| < 5 \times 10^{-7}$. At stronger wind stresses the wind-driven along-shelf currents are stronger than the tidal currents and consequently a quadratic drag law is more appropriate than the linear drag law used in the ATW model.

The ATW model reproduces the along-coast pressure gradient along both the New England and Central MAB coasts as well as a multiple regression analysis of the form

$$\frac{\partial\eta^P}{\partial y} = a\frac{1}{\sqrt{\pi}}\frac{\tau^{sy}_{\mathrm{GB}}}{\rho g D_{\mathrm{ATW}}} + b\frac{1}{\sqrt{\pi}}\frac{\tau^{sy}_{\mathrm{NE}}}{\rho g D_{\mathrm{ATW}}} + c\frac{1}{\sqrt{\pi}}\frac{\tau^{sy}_{\mathrm{CMAB}}}{\rho g D_{\mathrm{ATW}}} + d \qquad (4)$$

where, for example, τ^{sy}_{GB} is a representative along-coast wind stress for the southern flank of Georges Bank (Table 1). This indicates that the ATW is accurately reproducing the along-shelf pressure gradient response to the local and remote, poleward along-shelf wind stresses.

The substantially higher correlations between the observed and ATW model along-coast pressure gradients relative to only the local wind stress for the Central MAB suggests remote forcing is important along this section of coast. The contributions of the local and remote (poleward) along-shelf wind stresses to the along-coast pressure gradient in each region is determined by forcing the ATW model with wind stresses only along Georges Bank, only along the New England shelf, and only along the Central MAB shelf.

The pressure gradient along the New England coast from the ATW model is forced almost entirely by the local wind stress (97%–98% of forcing variance for daily, monthly, or yearly time scales), with a small (2%–3%) contribution from the Georges Bank wind stress (Figure 8a compare red and blue lines). The Georges Bank wind stress slightly reduces the response to the New England wind stress.

As anticipated, the pressure gradient along the Central MAB coast has significant contributions from both the local, Central MAB along-shelf wind stress (81% daily, 72% monthly, 85% yearly) and the remote, New England, along-shelf wind stress (18% daily, 27% monthly, 14% yearly) (Figure 8b). The Georges Bank wind stress contributes less than 1% of the forcing variance to the Central MAB along-coast pressure gradient. The larger percentage from the New England wind stress at monthly time scales relative to daily or yearly time scales is due to the notable contribution to the annual cycle of the Central MAB along-coast pressure gradient (Figure 8b blue line). Remote forcing is more important to the Central MAB along-coast pressure gradient because the wind stress along the New England coast is stronger than along the Central MAB coast (the standard deviation is 1.7 times larger). In contrast, wind stresses along the Southern Flank of Georges Bank are slightly weaker (87%) than wind stresses along the New England coast. The relative contributions of local versus remote forcing are essentially the same at daily time scales in both regions. In general, remote forcing has a stronger impact on coastal sea level (Lentz, 2024) than it does on along-coast pressure gradients in the MAB.

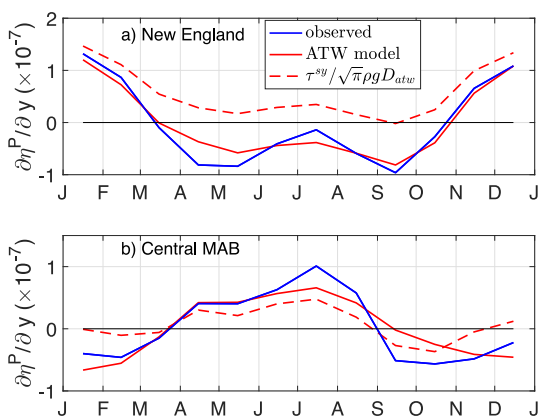

Figure 6. Annual cycles of the monthly observed and ATW model along-coast pressure gradients for the (a) New England and (b) Central Middle Atlantic Bight shelves. Annual cycles of the scaled along-shelf wind stress are also shown (dashed lines).

In the Southern MAB, where there are not enough tide gauges to estimate the along-shelf pressure gradient, the ATW model suggests that about 87% of the along-shelf pressure gradient response is due to the local along-shelf wind

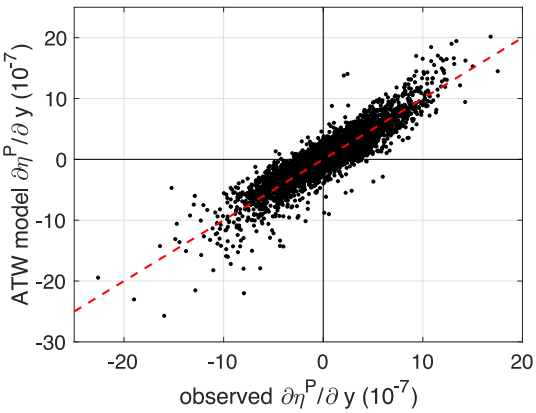

Figure 7. Scatter plot of daily observed versus ATW model along-coast pressure gradients for the New England shelf. Red dashed line has a slope of 1. Relationship is similar for Central Middle Atlantic Bight.

stress, with 10% from the Central MAB along-shelf wind stress and 3% from the New England along-shelf wind stress.

4.3. Dynamical Significance of the Along-Shelf Pressure Gradient

The observed along-coast pressure gradients are a significant component of the wind-driven dynamics over the inner shelf. The steady, barotropic, linear, depth-average along-shelf momentum balance used in the ATW model is

$$fhu_{da} = -gh\frac{\partial\eta^P}{\partial y} + \frac{\tau^{sy}}{\rho_o} - \frac{\tau^{by}}{\rho_o} \quad (5)$$

Here u_{da} is the depth-average cross-shelf current, $h(x)$ is the water depth, and τ^{sy} and τ^{by} are the along-shelf components of the surface wind stress and bottom stress. The size of the along-shelf pressure gradient term relative to the wind stress term depends on the water depth and the cross-shelf variations in the pressure gradient and wind stress terms. The ATW model suggests the wind-driven along-shelf pressure gradient is relatively constant over the inner shelf, defined in this case as $h(x) < D_{\mathrm{ATW}}$. The standard deviation of the observed along-coast pressure gradient term (at the coastal wall, $h_c = 15$ m) is 27% and 35% of the mid-shelf wind stress term along the New England and Central MAB coasts for daily averages, 34% and 42% for monthly averages and 54% and 49% for yearly averages. However, along-shelf wind stresses from buoys and towers closer to the coast are weaker than mid-shelf ERA5 wind stresses by about 60%. Consequently, the coastal pressure gradient term ($h_c = 15$ m) is generally 50%–80% of the local along-shelf wind stress term over the inner shelf. This tendency for the along-coast pressure gradient term to be a substantial fraction of the along-shelf wind stress term is consistent with previous studies of the along-shelf momentum balance at several MAB inner shelf sites at daily (Fewings & Lentz, 2010; Lentz et al., 1999; Masse, 1988; Ofsthun et al., 2019; Pettigrew, 1981) and monthly (Lentz, 2022) time scales.

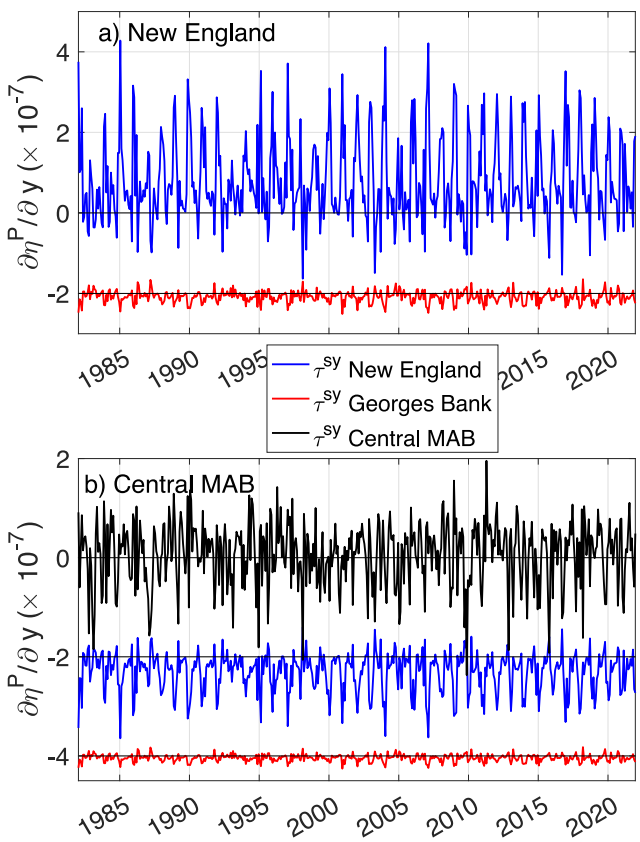

Figure 8. Relative contributions from monthly local and remote wind forcing to the ATW model estimates of the pressure gradient along the (a) New England and (b) Central Middle Atlantic Bight coasts.

5. Discussion

The magnitudes of the pressure gradient along the New England coast at daily and monthly time scales and the strong correlation with the along-shelf wind stress are consistent with the early studies based on more limited data sets (Beardsley & Butman, 1974; Beardsley et al., 1977; Chase, 1979; Noble & Butman, 1979; Wang, 1979). Bennett and Magnell (1979) argued that along-shelf pressure gradients on the New England shelf were set up by the water piling up in the corner of the New York Bight and setting up an opposing pressure gradient (see also Wang, 1979). The ATW model as implemented assumes a straight coastline and isobaths with abrupt changes in the wind stress at Great South Channel (east of Nantucket), the New York Bight (Sandy Hook), and Chesapeake Bay. While the abrupt change in coastline orientation undoubtedly has some impact on the pressure field, the success of the ATW model indicates that the primary cause of the wind-driven along-coast pressure gradients is along-shelf variations in the along-shelf component of the wind stress, not topographic constraints on the flow.

The relationship between the along-shelf wind stress and along-coast pressure gradient is also similar to results of a previous analysis for the region poleward of the MAB, the Gulf of Maine and Scotian shelf (Li et al., 2014). The ATW model provides a dynamically based depth scale, D_{ATW} (Equation 2), relating the along-shelf wind stress and the pressure gradient that should be applicable to other regions (e.g., Li et al., 2014). D_{ATW} is the water depth scale corresponding to the offshore spread of the wind-forced response and

depends on four parameters: the linear drag coefficient, the bottom slope, Coriolis, and an along-shelf scale for the wind stress.

The local and remote along-shelf wind stresses included in this study account for more than half of the along-coast pressure gradient variance in the MAB at time scales from days to months and more than 25% of the variance at yearly time scales. This is probably a conservative estimate given uncertainties in the sea-level observations, the reanalysis wind stresses, and the along-coast pressure gradient estimates. For example, differences between adjacent tide gauges that are relatively close together (e.g., Sandy Hook and Battery or Montauk and New London Figure 1) have standard deviations of ∼2 cm at daily, ∼1.5 cm at monthly and ∼1 cm at yearly time scales. These standard deviations are about 15% of the sea-level differences spanning the length of the New England (Nantucket to Sandy Hook) and Central MAB (Sandy Hook to Chesapeake Bay) coasts at daily and monthly time scales, but about 40% at yearly time scales. This undoubtedly contributes to the lower correlations between the observed and ATW model along-shelf pressure gradient at yearly time scales relative to daily and monthly time scales (Table 1).

The direct dynamical link between the regional along-shelf wind stress and the along-coast sea level gradient supports previous work suggesting that intermittent linkages between the North Atlantic Oscillation index and coastal sea level are due to shifts in the relationship between the NAO and local wind stress in the MAB region (e.g., Andres et al., 2013; Kenigson et al., 2018). For the 40 years time period examined here, both the along-shelf wind stresses and the pressure gradients along the New England and Central MAB coasts are uncorrelated with the NAO at monthly and yearly time scales.

It is surprising that the ATW model implementation represents the observed along-coast pressure gradients so well (Table 1, Figures 2–6) given the simplified dynamics and limitations in the implementation of the model. The model bathymetry with no along-shelf variation, a coastal wall, and a constant shelf bottom slope clearly neglects a number of bathymetric features that may be important, including substantial changes in the shelf width, the lack of a coast at the crest of Georges Bank, the sharp change in coastline orientation in the New York Bight, and features like Great South Channel between the New England shelf and Georges Bank (Figure 1). The use of a linear drag law is not accurate during strong forcing events at daily time scales (Figure 7) and surface gravity wave enhancements of the bottom stress are not considered (e.g., Lentz, 2022; Ofsthun et al., 2019). The model also does not include density variations, notably stratification which is substantial during the summer in the MAB and undoubtedly influences the dynamics.

At daily time scales, the steady-state assumption is not accurate, particularly over the mid and outer shelf, where the acceleration term in the along-shelf momentum balance can be significant (e.g., Shearman & Lentz, 2003). The ATW model does not include coastal trapped waves that propagate rapidly (order 7 m/s) equatorward along the MAB shelf and hence contribute to the response from remote, as well as local, wind forcing and are a significant contributor to a long-coast pressure gradients (e.g., Brunner et al., 2019; Noble et al., 1983; Ou et al., 1981; Schulz et al., 2012; Wang, 1979).

A major shortcoming of the implementation of the ATW model is the neglect of wind stress (and buoyancy) forcing in the Gulf of Maine and farther poleward. As noted in Section 2 the choice to only extend the model poleward over the Southern Flank of Georges Bank was to maintain the simplicity of the model and avoid the complex geometry and wind-driven response of the Gulf of Maine. Nevertheless, along-shelf wind stresses in the Gulf of Maine and over the Scotian shelf generate along-coast pressure gradients in those regions (Li et al., 2014) and probably contribute to the along-shelf pressure gradients in the MAB based on previous studies of sea level (e.g., Noble & Butman, 1979; Wang et al., 2022).

Offshore forcing may also contribute to sea level variability, and possibly along-coast pressure gradients, particularly from farther north in the Subpolar Gyre and at longer time scales (e.g., Frederiskse et al., 2017; Wise et al., 2018). There is substantial evidence for a "mean" along-shelf pressure gradient that drives the mean along-shelf flow in the MAB (e.g., Lentz, 2008; Scott & Csanady, 1976), that is not accounted for by the ATW model implementation in this study. Recent numerical modeling studies indicate the "mean" pressure gradients are driven by remote wind stress and buoyancy forcing over the eastern Canadian shelf and even farther poleward over the Greenland shelf (Chen & Yang, 2024; Pringle, 2018; Yang & Chen, 2021).

Other processes will also drive along-shelf pressure gradients at shorter scales, not resolved by the regional along-shelf pressure gradient estimates. Discharge from rivers and estuaries form buoyant plumes that propagate

equatorward along the MAB coast. Notable examples are the Hudson River, Delaware Bay and Chesapeake Bay (e.g., Chant et al., 2008; Münchow & Garvine, 1993; Rennie et al., 1999). The associated along-shelf pressure gradients can be substantial (e.g., Lentz et al., 1999). The Hudson and Delaware Bay plumes may contribute to the lower correlations between the observed and ATW model wind-forced pressure gradient along the Central MAB coast relative to the New England coast (Table 1). Surface gravity waves and cross-shelf wind stresses also drive coastal setup/setdown, primarily in the surf zone and inner shelf respectively (e.g., Lentz & Fewings, 2012). The setup and associated along-shelf pressure gradients are sensitive to the coastal geometry at individual tide gauges (Figure 1) and likely contribute to shorter scale "noise" in the regional scale along-shelf pressure gradient estimates.

6. Summary

Along-shelf wind stresses drive substantial along-coast variations in sea level and dynamically significant pressure gradients in the MAB at time scales from days to years. Sea-level differences along the New England (Nantucket to Sandy Hook, Figure 1) and Central MAB coasts (Sandy Hook to Chesapeake Bay) often exceed 20 cm at daily time scales (e.g., Figure 3) and occasionally 50 cm during strong storms (e.g., Figure 4). Sea-level differences often exceeded 5 cm and occasionally 10 cm at monthly time scales (Figure 5) and are 1–2 cm at yearly time scales. The associated wind-driven along-coast pressure gradients are a significant component of the dynamics over the inner-shelf (water depths of 5–30 m), typically 50%–80% of the wind stress in 15 m of water (inner-shelf wind stress magnitudes are about half mid-shelf wind stresses in the MAB).

The Arrested Topographic Wave model (Csanady, 1978) accurately reproduces the observed along-coast pressure gradients in the MAB (Table 1, Figures 3–7) and provides insight into the dynamics and the parameter dependence. The ATW model shows that the along-coast pressure gradient forced by the local along-shelf wind stress scales as $\partial\eta_P/\partial y \approx \tau^{sy}/\sqrt{\pi\rho g D_{\mathrm{ATW}}}$ (Equation 3b; Table 1), where D_{ATW} (Equation 2) depends on the linear drag coefficient, the bottom slope, the Coriolis frequency, and a characteristic along-shelf length scale for the wind stress. The ATW model also provides insight into the relative importance of local and remote along-shelf wind forcing. Pressure gradients along the New England coast are primarily driven by the local wind stress along the New England shelf (Figure 8a). In contrast, pressure gradients along the Central MAB coast are driven by both local along-shelf wind stresses and remote wind stresses along the New England shelf (Figure 8b). The success of the ATW model in accurately reproducing the observed along-coast pressure gradients in the MAB, suggests it is a useful model for broad shallow shelves that have a more barotropic response. It also raises the question of how useful the ATW model might be for narrower, steeper shelves where stratification may be more dynamically important, such as the west coast of the United States.

Data Availability Statement

The hourly tide gauge sea-level data are from the Center for Operational Oceanographic Products and Services (CO-OPS) (2018). CO-OPS Water Level Data from the Coastal Tide Gauge and Great Lake Water Level Network of the United States and US Territories. NOAA National Centers for Environmental Information. https://doi.org/10.25921/dt9g-2p60 [accessed 2 May 2022 via https://tidesandcurrents.noaa.gov/stations.html?type=Historic+Water+Levels]. The ERA5 wind stresses and atmospheric pressures are from the European Centre For Medium-Range Weather Forecasts (2019), updated monthly. *ERA5 Reanalysis (0.25 Degree Latitude-Longitude Grid)*. Research Data Archive at the National Center for Atmospheric Research, Computational and Information Systems Laboratory. https://doi.org/10.5065/BH6N-5N20. Accessed 14 December 2022.

Acknowledgments
The author thanks Ken Brink and two anonymous reviewers for helpful suggestions on an early draft of this manuscript. The analysis presented here was partially funded by the National Science Foundation under grants OCE #2219670 and OCE #2322676 (LTER Phase II).

References

Allen, J. S., & Smith, R. L. (1981). On the dynamics of wind-driven shelf currents. *Philosophical Transactions of the Royal Society London A*, *302*, 617–634.

Andres, M., Gawarkiewicz, G. G., & Toole, J. M. (2013). Interannual sea level variability in the western North Atlantic: Regional forcing and remote response. *Geophysical Research Letters*, *40*(22), 5915–5919. https://doi.org/10.1002/2013GL058013

Beardsley, R. C., & Butman, B. (1974). Circulation on the New England continental shelf: Response to strong winter storms. *Geophysical Research Letters*, *1*(4), 181–184. https://doi.org/10.1029/gl001i004p00181

Beardsley, R. C., Mofjeld, H., Wimbush, M., Flagg, C. N., & Vermersch, J. A. (1977). Ocean tides and weather-induced bottom pressure fluctuations in the Middle-Atlantic Bight. *Journal of Geophysical Research*, *82*(21), 3175–3182. https://doi.org/10.1029/jc082i021p03175

Bennett, J. R., & Magnell, B. A. (1979). A dynamical analysis of currents near the New Jersey coast. *Journal of Geophysical Research*, *84*(C3), 1165–1175. https://doi.org/10.1029/jc084ic03p01165

Brink, K. H. (1991). Coastal-trapped waves and wind-driven currents over the continental shelf. *Annual Reviews of Fluid Mechanics*, *23*(1), 389–412. https://doi.org/10.1146/annurev.fl.23.010191.002133

Brown, W. S., Irish, J. D., & Winant, C. D. (1987). A description of subtidal pressure field observations on the northern California continental shelf during the Coastal Ocean Dynamics Experiment. *Journal of Geophysical Research*, *92*(C2), 1605–1636. https://doi.org/10.1029/jc092ic02p01605

Brunner, K., Rivas, D., & Lwiza, K. M. M. (2019). Application of classical coastal trapped wave theory to high-scattering regions. *Journal of Physical Oceanography*, *49*(9), 2201–2216. https://doi.org/10.1175/JPO-D-18-0112.1

Center for Operational Oceanographic Products and Services (CO-OPS). (2018). *CO-OPS water level data from the coastal tide gauge and great lake water level network of the United States and US Territories*. NOAA National Centers for Environmental Information. https://doi.org/10.25921/dt9g-2p60

Chant, R. J., Wilkin, J., Zhang, W., Choi, B.-J., Hunter, E., Castelao, R., et al. (2008). Dispersal of the Hudson River Plume in the New York Bight: Synthesis of observational and numerical studies during LaTTE. *Oceanography*, *21*(4), 148–161. https://doi.org/10.5670/oceanog.2008.11

Chase, R. R. P. (1979). The coastal longshore pressure gradient: Temporal variations and driving mechanisms. *Journal of Geophysical Research*, *84*(C8), 4898–4904. https://doi.org/10.1029/jc084ic08p04898

Chen, K., & Yang, J. (2024). What drives the mean along-shelf flow in the Northwest Atlantic coastal ocean? *Journal of Geophysical Research: Oceans*, *129*(7), e2024JC021079. https://doi.org/10.1029/2024JC021079

Csanady, G. T. (1978). The arrested topographic wave. *Journal of Physical Oceanography*, *8*(1), 47–62. https://doi.org/10.1175/1520-0485(1978)008<0047:tatw>2.0.co;2

European Centre For Medium-Range Weather Forecasts. (2019). ERA5 reanalysis (0.25 degree latitude-longitude grid) [Dataset]. *UCAR/NCAR - Research Data Archive*. https://doi.org/10.5065/BH6N-5N20

Fewings, M. R., & Lentz, S. J. (2010). Momentum balances on the inner continental shelf at Martha's Vineyard Coastal Observatory. *Journal of Geophysical Research*, *115*(12). https://doi.org/10.1029/2009JC005578

Frederikse, T., Simon, K., Katsman, C. A., & Riva, R. (2017). The sea-level budget along the Northwest Atlantic coast: GIA, mass changes, and large-scale ocean dynamics. *Journal of Geophysical Research: Oceans*, *122*(7), 5486–5501. https://doi.org/10.1002/2017JC012699

Greenberg, D., Loder, J., Shen, Y., Lynch, D., & Naimie, C. (1997). Spatial and temporal structure of the barotropic response of the Scotian Shelf and Gulf of Maine to surface wind stress: A model-based study. *Journal of Geophysical Research*, *102*(C9), 20897–20915. https://doi.org/10.1029/97jc00442

Gutierrez, B. T., Voulgaris, G., & Work, P. A. (2006). Cross-shore variations of wind-driven flows on the inner shelf in Long Bay, South Carolina, United States. *Journal of Geophysical Research*, *111*(C3), C03015. https://doi.org/10.1029/2005jc003121

Hersbach, H., Bell, B., Berrisford, P., Biavati, G., Horányi, A., Muñoz Sabater, J., et al. (2023). ERA5 hourly data on single levels from 1940 to present. *Copernicus Climate Change Service (C3S) Climate Data Store (CDS)*. https://doi.org/10.24381/cds.adbb2d47

Hickey, B. M. (1984). The fluctuating longshore pressure gradient on the Pacific Northwest shelf: A dynamical analysis. *Journal of Physical Oceanography*, *14*(2), 276–293. https://doi.org/10.1175/1520-0485(1984)014,0276:TFLPGO.2.0.CO;2

Hickey, B. M., Dobbins, E. L., & Allen, S. E. (2003). Local and remote forcing of currents and temperature in the central Southern California Bight. *Journal of Geophysical Research*, *108*(C3), C3081. https://doi.org/10.1029/2000jc000313

Hickey, B. M., & Pola, N. E. (1983). The seasonal alongshore pressure gradient on the west coast of the United States. *Journal of Geophysical Research*, *88*(C12), 7623–7633. https://doi.org/10.1029/JC088iC12p07623

Kenigson, J. S., Han, W., Rajagopalan, B., Yanto, & Jasinski, M. (2018). Decadal shift of NAO-linked interannual sea level variability along the U. S. Northeast coast. *Journal of Climate*, *31*(13), 4981–4989. https://doi.org/10.1175/JCLI-D-17-0403.1

Kirincich, A. R., & Barth, J. A. (2009). Along-shelf variability of inner-shelf circulation along the Central Oregon coast during summer. *Journal of Physical Oceanography*, *39*(6), 1380–1398. https://doi.org/10.1175/2008jpo3760.1

Lee, T. N., Ho, W. J., Kourafalou, V., & Wang, J. D. (1984). Circulation on the continental shelf of the southeastern United States. Part I: Subtidal response to wind and Gulf Stream forcing during winter. *Journal of Physical Oceanography*, *14*(6), 1001–1012. https://doi.org/10.1175/1520-0485(1984)014<1001:cotcso>2.0.co;2

Lee, T. N., Williams, E., Wang, R. E. J., & Atkinson, L. (1989). Response of South Carolina continental shelf waters to wind and Gulf Stream forcing during winter of 1986. *Journal of Geophysical Research*, *94*(C8), 10715–10754. https://doi.org/10.1029/jc094ic08p10715

Lentz, S. J. (1994). Current dynamics over the northern California inner shelf. *Journal of Physical Oceanography*, *24*(12), 2461–2478. https://doi.org/10.1175/1520-0485(1994)024<2461:cdotnc>2.0.co;2

Lentz, S. J. (2008). Observations and a model of the mean circulation over the Middle Atlantic Bight continental shelf. *Journal of Physical Oceanography*, *38*(6), 1203–1221. https://doi.org/10.1175/2007jpo3768.1

Lentz, S. J. (2022). Inter-annual and seasonal along-shelf current variability and dynamics – Seventeen years of observations from the southern New England inner shelf. *Journal of Physical Oceanography*, *52*(12), 2923–2933. https://doi.org/10.1175/JPO-D-22-0064.1

Lentz, S. J. (2024). The coastal sea-level response to wind stress in the Middle Atlantic Bight. *Journal of Geophysical Research: Oceans*, *129*(8). https://doi.org/10.1029/2024JC021269

Lentz, S. J., & Fewings, M. R. (2012). The wind-and wave-driven inner-shelf circulation. *Annual Reviews of Marine Science*, *4*(1), 317–343. https://doi.org/10.1146/annurev-marine-120709-142745

Lentz, S. J., Guza, R. T., Elgar, S., Feddersen, F., & Herbers, T. H. C. (1999). Momentum balances on the North Carolina inner shelf. *Journal of Geophysical Research*, *104*(C8), 18205–18226. https://doi.org/10.1029/1999jc900101

Lentz, S. J., & Winant, C. D. (1986). Subinertial currents on the southern California shelf. *Journal of Physical Oceanography*, *16*(11), 1737–1750. https://doi.org/10.1175/1520-0485(1986)016<1737:scotsc>2.0.co;2

Li, Y., Ji, R., Fratantoni, P. S., Chen, C., Hare, J. A., Davis, C. S., & Beardsley, R. C. (2014). Wind-induced interannual variability of sea level slope, along-shelf flow, and surface salinity on the Northwest Atlantic shelf. *Journal of Geophysical Research: Oceans*, *119*(4), 2462–2479. https://doi.org/10.1002/2013JC009385

Liu, Y., & Weisberg, R. H. (2005). Momentum balance diagnoses for the West Florida Shelf. *Continental Shelf Research*, *25*(17), 2054–2074. https://doi.org/10.1016/j.csr.2005.03.004

Masse, A. K. (1988). *Estuary-shelf interaction: Delaware Bay and the inner shelf* (Ph.D. thesis) (p. 216). University of Delaware.

McCabe, R. M., Hickey, B. M., Dever, E. P., & MacCready, P. (2015). Seasonal cross-shelf flow structure, upwelling relaxation, and the along-shelf pressure gradient in the Northern California Current system. *Journal of Physical Oceanography*, *45*(1), 209–227. https://doi.org/10.1175/JPO-D-14-0025.1

Münchow, A., & Garvine, R. W. (1993). Dynamical properties of a buoyancy-driven coastal current. *Journal of Geophysical Research*, *98*(C11), 20063–20077. https://doi.org/10.1029/93jc02112

Noble, M., & Butman, B. (1979). Low-frequency wind-induced sea level oscillations along the east coast of North America. *Journal of Geophysical Research*, *84*(C6), 3227–3236. https://doi.org/10.1029/jc084ic06p03227

Noble, M., Butman, B., & Williams, E. (1983). On the longshelf structure and dynamics of subtidal currents on the eastern United States continental shelf. *Journal of Physical Oceanography*, *13*(12), 2125–2147. https://doi.org/10.1175/1520-0485(1983)013<2125:otlsad>2.0.co;2

Noble, M., Butman, B., & Wimbush, M. (1985). Wind-current coupling on the southern flank of Georges Bank—Variation with season and frequency. *Journal of Physical Oceanography*, *15*(5), 604–620. https://doi.org/10.1175/1520-0485(1985)015<0604:wcotsf>2.0.co;2

Noble, M. A., Ryan, H. F., & Wiberg, P. L. (2002). The dynamics of subtidal poleward flows over a narrow continental shelf, Palos Verdes, CA. *Continental Shelf Research*, *22*(6–7), 923–944. https://doi.org/10.1016/s0278-4343(01)00112-1

Ofsthun, C., Wu, X., Voulgaris, G., & Warner, J. C. (2019). Alongshore momentum balance over shoreface-connected ridges, Fire Island, NY. *Continental Shelf Research*, *186*, 21–33. https://doi.org/10.1016/j.csr.2019.07.005

Ou, H. W., Beardsley, R. C., Mayer, D., Boicourt, W. C., & Butman, B. (1981). An analysis of subtidal current fluctuations in the Middle Atlantic Bight. *Journal of Physical Oceanography*, *11*(10), 1383–1392. https://doi.org/10.1175/1520-0485(1981)011<1383:aaoscf>2.0.co;2

Pettigrew, N. R. (1981). *The dynamics and kinematics of the coastal boundary layer off Long Island* (Ph.D. thesis) (p. 262). Woods Hole Oceanogr. Inst., Woods Hole.

Pringle, J. M. (2006). Sources of variability in Gulf of Maine circulation, and the observations needed to model it. *Deep-Sea Research II*, *53*(23–24), 2457–2476. https://doi.org/10.1016/j.dsr2.2006.08.015

Pringle, J. M. (2018). Remote forcing of shelf flows by density gradients and the origin of the annual mean flow on the Mid-Atlantic Bight. *Journal of Geophysical Research: Oceans*, *123*(7), 4464–4482. https://doi.org/10.1029/2017JC013721

Rennie, S. E., Largier, J. L., & Lentz, S. J. (1999). Observations of a pulsed buoyancy current downstream of Chesapeake Bay. *Journal of Geophysical Research*, *104*(C8), 18227–18240. https://doi.org/10.1029/1999JC900153

Schulz, W. J., Mied, R. P., & Snow, C. M. (2012). Continental shelf wave propagation in the Mid-Atlantic Bight: A general dispersion relation. *Journal of Physical Oceanography*, *42*(4), 558–568. https://doi.org/10.1175/JPO-D-11-098.1

Scott, J. T., & Csanady, G. T. (1976). Nearshore currents off Long Island. *Journal of Geophysical Research*, *81*(30), 5401–5409. https://doi.org/10.1029/jc081i030p05401

Shearman, R. K., & Lentz, S. J. (2003). Dynamics of mean and subtidal flow on the New England Shelf. *Journal of Geophysical Research*, *108*(C8), 3281. https://doi.org/10.1029/2002JC001417

Wang, D. P. (1979). Low-frequency sea level variability on the Middle Atlantic Bight. *Journal of Marine Research*, *37*, 683–696.

Wang, O., Lee, T., Piecuch, C. G., Fukumori, I., Fenty, I., Frederikse, T., et al. (2022). Local and remote forcing of interannual sea-level variability at Nantucket Island. *Journal of Geophysical Research: Oceans*, *127*(6), e2021JC018275. https://doi.org/10.1029/2021JC018275

Wise, A., Hughes, C. W., & Polton, J. (2018). Bathymetric influence on the coastal sea level response to ocean gyres at western boundaries. *Journal of Physical Oceanography*, *48*(12), 2949–2964. https://doi.org/10.1175/JPO-D-18-0007.1

Wright, D. G., Greenberg, D. A., Loder, J. W., & Smith, P. C. (1986). The steady-state barotropic response of the Gulf of Maine and adjacent regions to surface wind stress. *Journal of Physical Oceanography*, *16*(5), 947–966. https://doi.org/10.1175/1520-0485(1986)016<0947:tssbro>2.0.co;2

Yang, J., & Chen, K. (2021). The role of wind stress in driving the along-shelf flow in the northwest Atlantic Ocean. *Journal of Geophysical Research: Oceans*, *126*(4), e2020JC016757. https://doi.org/10.1029/2020JC016757